

## Supplementary Information

### Characterization of the DNA duplex unzipping through a sub-2 nm solid-state nanopore

Yao Lin<sup>a†</sup>, Xin Shi<sup>a†</sup>, Shao-Chuang Liu<sup>a†</sup>, Yi-Lun Ying<sup>a\*</sup>, Qiao Li<sup>a</sup>, Rui Gao<sup>a</sup>, Farkhondeh Fathi<sup>b</sup>, Yi-Tao Long<sup>a\*</sup>, He Tian<sup>a</sup>

<sup>a</sup>School of Chemistry and Molecular Engineering, East China University of Science and Technology, 130 Meilong Road, Shanghai, 200237, P. R. China.

Tel./fax: +86 021-64250032

\*E-mail: yilunying@ecust.edu.cn; ytlong@ecust.edu.cn

<sup>b</sup>Department of Chemistry and Biochemistry, Mount Allison University, 63C York Street, Sackville, NB, E4L 3G4, Canada.

† These authors contributed equally to this work

## Experimental Section

### 1. Reagents and materials.

Potassium chloride (KCl,  $\geq 99.5\%$ ) was purchased from Sigma-Aldrich (St. Louis, MO, USA). Ethylenediaminetetraacetic acid (EDTA, 99.995%) and Tris (hydroxymethyl) aminomethane (Tris,  $\geq 99.9\%$ ) were purchased from Aladdin Reagent Co., Ltd. (Shanghai, China). Lithium Chloride (LiCl,  $\geq 99.7\%$ ) was purchased from the Sinopharm Chemical Reagent Company (Shanghai, China). The 50-nt ssDNA samples (5'-(dA)<sub>50</sub>-3') and DNA duplex samples were synthesized and HPLC-purified by Sangon Biotech Co., Ltd (Shanghai, PRC). The DNA duplex had the following sequence:



All reagents were of analytical grade. All solutions were prepared by Milli-Q ultrapure water with resistance of 18.2 M  $\Omega$  cm at 25 °C (EMD Millipore, Billerica, USA) and were filtered with 0.22- $\mu\text{m}$  pore-size filter (Rephile Bioscience Ltd., Shanghai, China).

### 2. Experimental setup and data acquisition.

The chip was sealed between two polytetrafluoroethylene (PTFE) flow cells using screws. Nanopore fabrications were performed in 1 M potassium chloride (KCl) containing 10 mM Tris-HCl and 1 mM EDTA at pH 10. DNA translocation studies were performed in 4 M Lithium Chloride (LiCl) containing 10 mM Tris-HCl and 1 mM EDTA at pH 8. Two Ag/AgCl electrodes were immersed into two electrolyte chambers respectively to apply a bias voltage and connected to a current amplifier. A custom-designed LabVIEW

software was used to acquire data with a DAQ card<sup>1</sup>. The voltage used to fabricate a nanopore was set by the DAQ card, and when the measured current exceeded the predetermined threshold current, voltage bias was terminated rapidly. Current traces were measured at a sampling rate of 100 kHz using Axopatch 200B (Axon Instruments, Forest City, USA) with a 5 kHz low-pass Bessel filter. Data analysis was performed using a home-designed software (<http://people.bath.ac.uk/yl505/nanoporeanalysis.html>) and Origin 9.2 (OriginLab Corporation, Northampton, USA). The number of analyzed ssDNA events is 552 and the number of typical signatures of Type II for DNA duplexes analyzed is 295. The error bar denotes standard error. The experiments of nanopore fabrication and DNA translocation were both carried out in a Faraday cage to shield electromagnetic noise. The transmission electron microscope (TEM) images of nanopores were obtained on a Tecnai G2 F20 S-TWIN transmission electron microscope (FEI, USA) operated at an accelerating voltage of 200 kV, Titan 80–300 scanning/transmission electron microscope (S/TEM) operated at 300 kV (FEI, USA) and JEM-2010 high-resolution transmission electron microscope (JEOL Ltd., Japan) operated at 200 kV.

### 3. Preparation of membranes.

Nanopores were fabricated in 10-nm low-stress silicon nitride transmission electron microscope (TEM) windows purchased from Norcada, Inc. (product # NT005Z, Alberta, CAN). Before fabrication of the pore, the membranes were cleaned and hydrophilised on each side with oxygen plasma for 30 s. The nanopores used to obtain TEM images were fabricated in 10-nm thick membranes with windows of 10  $\mu\text{m}$  by 10  $\mu\text{m}$ . For TEM imaging, the silicon nitride membrane were immersed in warm water for several hours to remove salt residues. This cleaning procedure may alter the pore dimensions.

### 4. Analysis of DNA duplex unzipping process using a conductance model.

In order to verify the whole unzipping process of DNA duplex, a conductance model is applied based on previous work<sup>2</sup>. The conductance change of the three levels are described as follows:

For level 1

$$\Delta G_1 = \left( \frac{1}{G_{acc\ dsDNA}} + \frac{1}{G_{pore\ dsDNA}} + \frac{1}{G_{acc\ ssDNA}} \right)^{-1} - G_{0\ Total} \quad (1)$$

$$G_{0\ Total} = \left( \frac{1}{G_{0\ pore}} + \frac{2}{G_{0\ acc}} \right)^{-1} \quad (2)$$

$$G_{acc\ dsDNA} = G_{0\ acc} - \sigma \frac{\pi d_{dsDNA}^2}{2d} = 2\sigma d - \sigma \frac{\pi d_{dsDNA}^2}{2d} = 2\sigma d - \sigma \frac{\pi d}{2} \quad (3)$$

Where  $d$  is nanopore diameter (1.6 nm) and  $\sigma$  is the conductivity of the solution (15.5 S  $\text{m}^{-1}$ ). Since the diameter of DNA duplex is larger than the pore, we assume that the diameter of the distorted DNA equals to pore's diameter. Similarly,  $G_{acc\ ssDNA} = 2\sigma d - \sigma \frac{\pi d_{ssDNA}^2}{2d}$ , where  $d_{ssDNA}$  is the diameter of ssDNA (1.4 nm).

$G_{pore dsDNA} = G_{0 pore} - G_{DNApore} = G_{0 pore} - \sigma \frac{\pi d_{dsDNA}^2}{4l} = \sigma \frac{\pi d^2}{4l} - \sigma \frac{\pi d_{dsDNA}^2}{4l}$  (4) Since we assume that  $d_{dsDNA} \approx d$ ,  $G_{pore dsDNA} \approx 0$ . As a result,  $\Delta G_1 \approx -G_{0 Total}$ , which means the DNA duplex unzipping inside the pore generates a nearly full blockade.

For level 2,

$$\Delta G_2 = \left( \frac{1}{G_{acc ssDNA}} + \frac{1}{G_{pore ssDNA}} + \frac{1}{G_{0 acc}} \right)^{-1} - G_{0 Total} \quad (5)$$

$$G_{pore ssDNA} = G_{0 pore} - G_{DNApore} = G_{0 pore} - \sigma \frac{\pi d_{ssDNA}^2}{4l} \quad (6)$$

For level 3,

$$\Delta G_3 = \left( \frac{2}{G_{acc ssDNA}} + \frac{1}{G_{pore ssDNA}} \right)^{-1} - G_{0 Total} \quad (7)$$

Although the conductance model can explain the DNA duplexes unzipping process in our experiments, some difference still exist between the calculated results and the experimental detection ones. The orientations of DNA duplex and the unzipped ssDNA dynamically changes when they are interacting with the pore, leading to the differences of the total conductance change.

Table S1. Comparison of the calculated results from the model with the experimental data.

		Level 1	Level 2	Level 3
<b>Theoretical data</b>	$\Delta G$	-5.6	-3.8	-4.3
	$\Delta I/I_0$	0.90	0.61	0.70
<b>Experimental data</b>	$\Delta G$	-6.2	-4.5	-4.7
	$\Delta I/I_0$	1.0	0.72	0.74

## 5. Calculation of the kinetic rate constant<sup>3</sup> of dissociation (k<sub>off</sub>) and association (k<sub>on</sub>)

k<sub>off</sub> and k<sub>on</sub> are related to the mean residence time (T<sub>t</sub>) and the mean inter-event time (T<sub>i</sub>) via k<sub>off</sub> (s<sup>-1</sup>) = 1/T<sub>t</sub>, and k<sub>on</sub> (M<sup>-1</sup>s<sup>-1</sup>) = 1/(cT<sub>i</sub>). c is the concentration of analyte. The dissociation constant is given by K<sub>d</sub> (M) = k<sub>off</sub>/k<sub>on</sub>, and the association constant is given by K<sub>a</sub> (M<sup>-1</sup>) = 1/K<sub>d</sub>. The concentration of DNA duplex we used is 5 uM. At 400 mV, T<sub>i</sub>= 22 ms, T<sub>t</sub>= 31 ms, as a result, k<sub>off</sub> = 32.3 s<sup>-1</sup>, and k<sub>on</sub>= 9.10 × 10<sup>6</sup> M<sup>-1</sup> s<sup>-1</sup>; and the corresponding dissociation constant, K<sub>d</sub>=7.04 × 10<sup>-6</sup> M, and association constant, K<sub>a</sub> = 1.42 × 10<sup>5</sup> M<sup>-1</sup>

Table S2. The parameters of exponential fitting

<b>Data</b>	<b>Function form</b>	<b>y0</b>	<b>A1</b>	<b>t1</b>	<b>k</b>	<b>tau</b>
Duration histogram of ssDNA (Figure 2b)	$y = A1 \cdot \exp(-x/t1) + y0$	0.51	216	0.20	5.3	0.13

Table S3. The parameters of Gaussian fitting

<b>Data</b>	<b>Function form</b>	<b>y0</b>	<b>xc</b>	<b>w</b>	<b>A</b>
Current histogram of poly(dA) <sub>50</sub> (Figure 2b)	$y = y0 + (A/(w \cdot \sqrt{\pi/2})) \cdot \exp(-2 \cdot ((x-xc)/w)^2)$	6.8	0.67	0.14	10
Duration histogram of Level 1 (Figure 3b)	$y = y0 + (A/(w \cdot \sqrt{\pi/2})) \cdot \exp(-2 \cdot ((x-xc)/w)^2)$	6.5	31	19	777
Current histogram of Level 1 (Figure 3c)	$y = y0 + (A/(w \cdot \sqrt{\pi/2})) \cdot \exp(-2 \cdot ((x-xc)/w)^2)$	1.9	0.90	0.030	3.9
Current histogram of Level 2 (Figure 3c)	$y = y0 + (A/(w \cdot \sqrt{\pi/2})) \cdot \exp(-2 \cdot ((x-xc)/w)^2)$	0.32	0.61	0.19	4.2
Current histogram of Level 3 (Figure 3c)	$y = y0 + (A/(w \cdot \sqrt{\pi/2})) \cdot \exp(-2 \cdot ((x-xc)/w)^2)$	2.1	0.70	0.13	3.0

Table S4. The parameters of linear fitting

<b>Data</b>	<b>Function form</b>	<b>a</b>	<b>b</b>
Relationship between duration time of Level 1 and the applied voltage (Figure 3d)	$y = a + b \cdot x$	3.5	-0.0050
Relationship between duration time of Level 3 and the applied voltage (Figure 3d,inset)	$y = a + b \cdot x$	-0.19	-0.0014

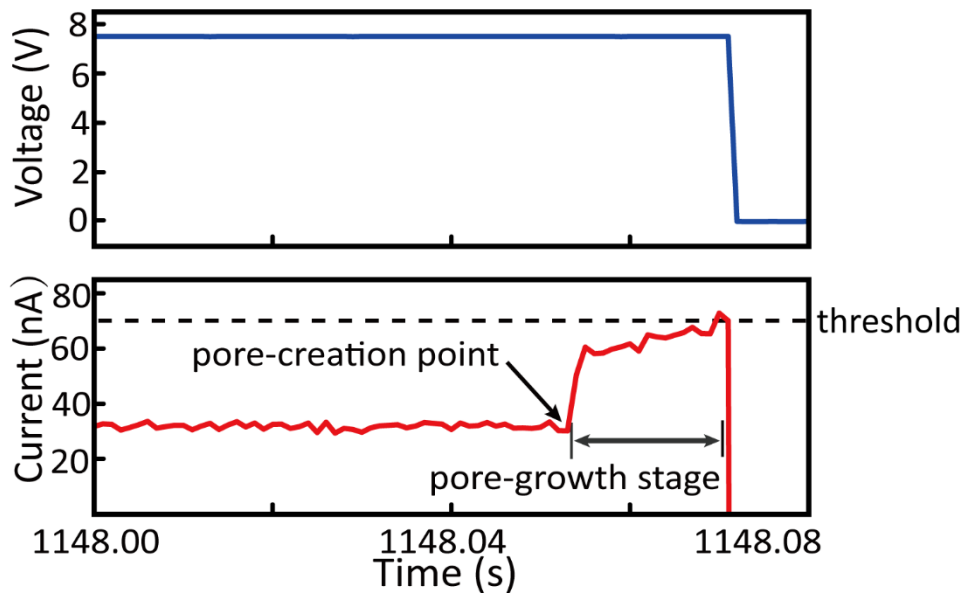


Figure S1. Leakage current at 7.5 V on a 10 nm SiN<sub>x</sub> membrane in 1 M KCl, 10 mM Tris, and 1mM EDTA (pH 10) solution. The nanopore is allowed to grow until a predetermined threshold current is reached, then the voltage is turned off at this point.

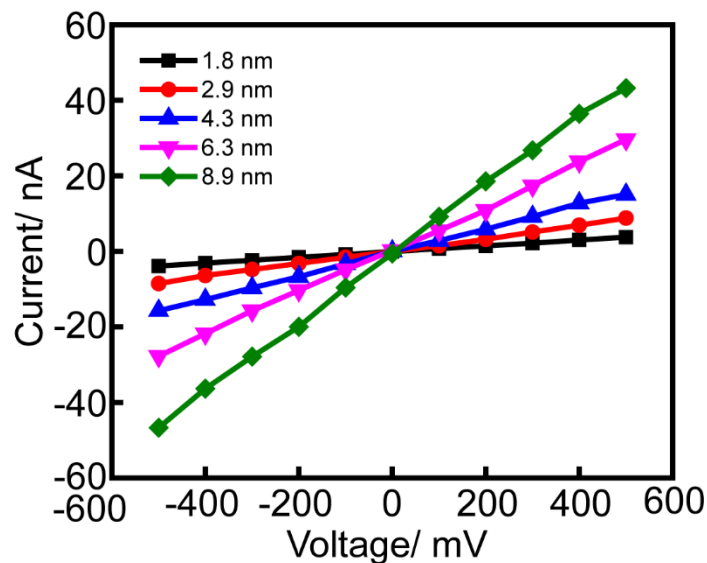


Figure S2. I-V curves of five fabricated nanopores measured in 4 M LiCl (pH 8). The diameters of the five pores are 1.8 nm, 2.9 nm, 4.3 nm, 6.3 nm and 8.9 nm corresponding to its conductance of 7.6 nS, 16.9 nS, 31.3 nS, 56.5 nS and 90.0 nS, respectively. All pores are equilibrated in 4 M LiCl (pH 8) for several hours until the pores are stable and not rectifying.

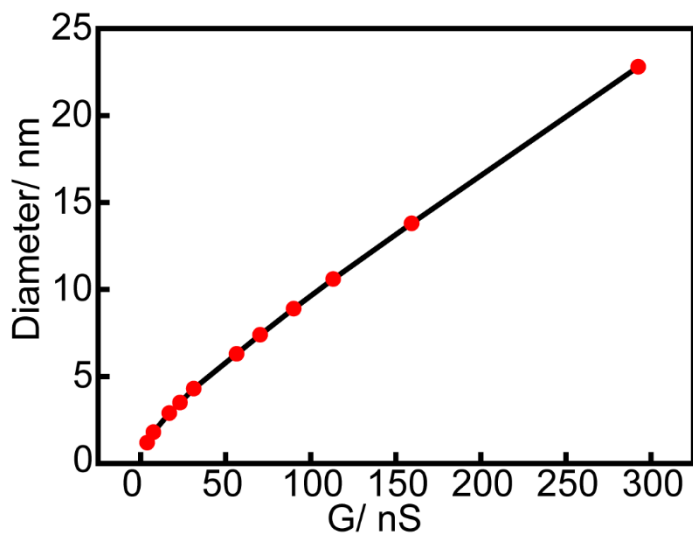


Figure S3. Relation between the diameters of the fabricated nanopores and conductance in 4 M LiCl solution.

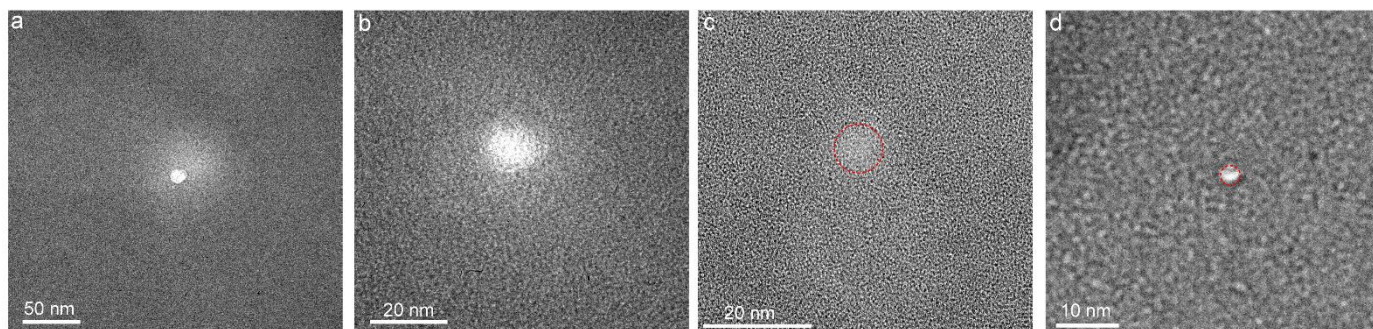


Figure S4. TEM images of nanopores fabricated by controlled dielectric breakdown. a) Image of a nanopore with diameter of  $\sim 12$  nm. Calculated pore size is 9.6 nm based on its conductance. b) Image of the nanopore shown in (a) at higher magnification. c) Image of nanopore with diameter of  $\sim 9$  nm. Calculated pore size is 6.8 nm based on its conductance. d) Image of nanopore with diameter of  $\sim 3$  nm. Calculated pore size is 1.8 nm based on its conductance.

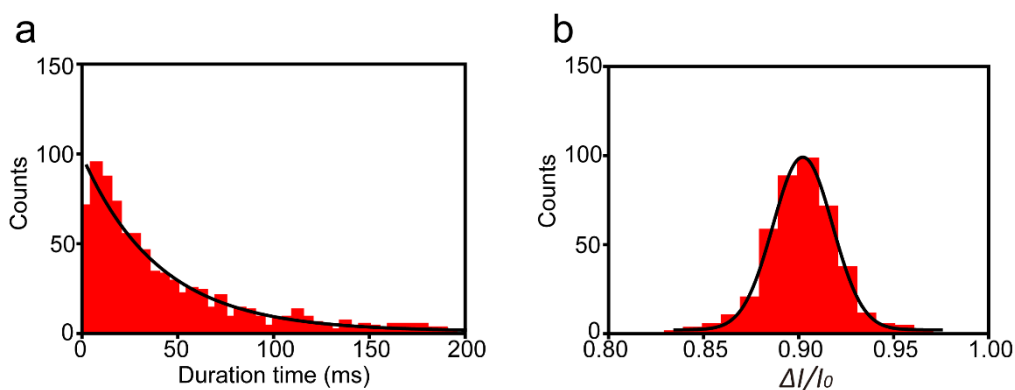


Figure S5. a) Histogram of duration time for type II events of DNA duplex. The histogram of duration time is fit to an exponential function. b) Histogram of current blockade ( $\Delta I/I_0$ ) for type II events. The histogram of  $\Delta I/I_0$  is fit to a Gaussian function. The applied potential set to 400 mV.

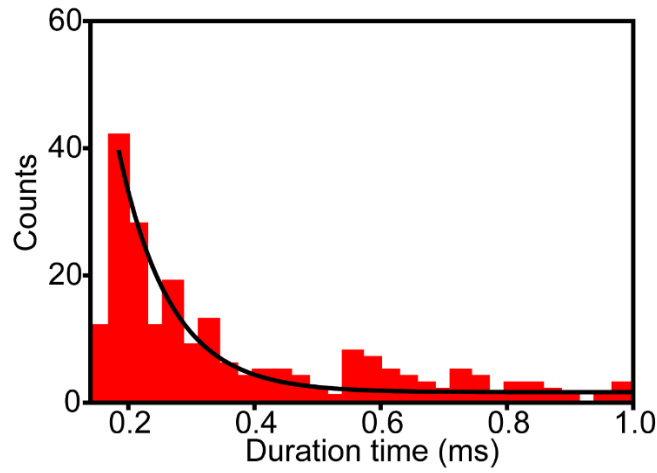


Figure S6. Histogram of duration time for Level 3 state. The histogram of duration time is fit to an exponential function.

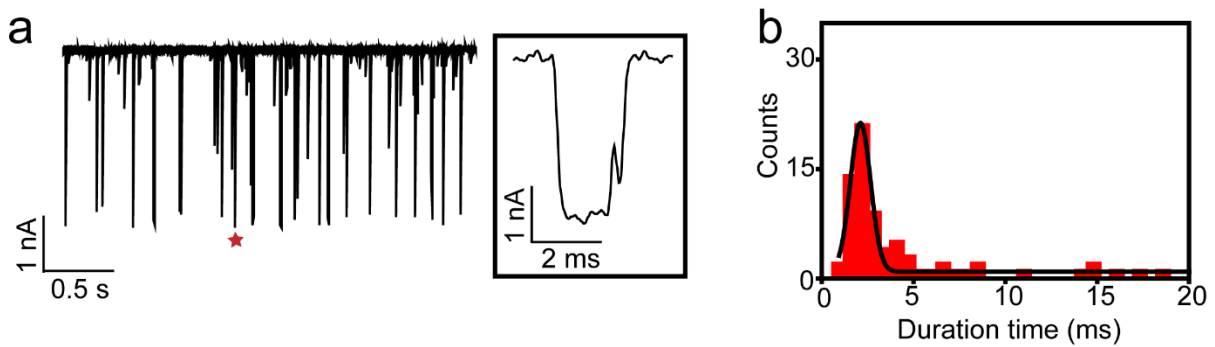


Figure S7. a) Current traces of DNA duplexes (40-bp duplex region and a 20-nt single-strand overhang) at applied voltage of 400 mV. Left insert: typical three-level current blockades. b) The histogram of duration time for DNA duplexes unzipping with sub-2-nm solid-state nanopore at 400 mV. The histogram of duration time is fit to a Gaussian function. The duration time is 2.2 ms which is shorter than that of the duplexes with a 10-nt overhang. This decrease is attributed to the strong driving force associated to the long overhang strand for DNA duplex unzipping process as described in previous studies<sup>4,5</sup>.

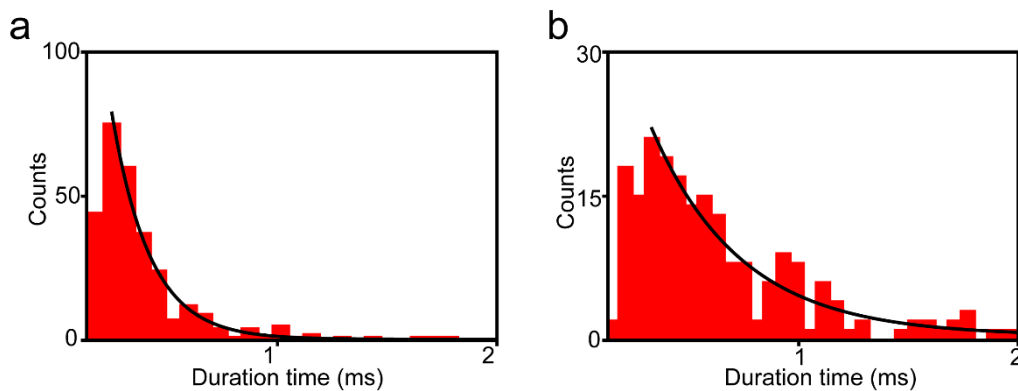


Figure S8. Analysis of DNA duplex and ssDNA translocation in an 8-nm solid-state nanopore. a) Histogram of duration time for ssDNA translocation events at 300 mV. b) Histogram of duration time for DNA duplex translocation events at 300 mV. The histograms of duration time are fit to exponential function. The duration

times of ssDNA and DNA duplex are 0.17 ms and 0.45 ms, respectively.

## References

- 1 H. Kwok, K. Briggs and V. Tabard-Cossa, *PLoS One*, 2014, **9**, e92880.
- 2 A. T. Carlsen, O. K. Zahid, J. Ruzicka, E. W. Taylor and A. R. Hall, *ACS Nano*, 2014, **8**, 4754–4760.
- 3 A. Oukhaled, L. Bacri, M. Pastoriza-Gallego, J.-M. Betton and J. Pelta, *ACS Chem. Biol.*, 2012, **7**, 1935–1949.
- 4 U. F. Keyser, B. N. Koeleman, S. van Dorp, D. Krapf, R. M. M. Smeets, S. G. Lemay, N. H. Dekker and C. Dekker, *Nat Phys*, 2006, **2**, 473–477.
- 5 Y. Wang, K. Tian, L. L. Hunter, B. Ritzo and L.-Q. Gu, *Nanoscale*, 2014, **6**, 11372–11379.